BULLETIN OF COMPUTER SCIENCE RESEARCH
ISSN 2774-3659 (Media Online)
Vol 6, No 2, February 2026 | Hal 585-593
https://hostjournals.com/bulletincsr
DOI: 10.47065/bulletincsr.v6i2.796

Lightweight Convolutional Neural Network Based on Modified LeNet for Retinal Pathology Classification in High-Resolution Fundus Imaging

Cahyatul Mu'awanah, Lukman Hakim*

Faculty of Engineering, Informatics Engineering Study Program, Universitas Yudharta, Pasuruan, Indonesia
Email: [1]cahyatulanna57372@gmail.com, [2,*]lukman@yudharta.ac.id
Correspondence Author Email: lukman@yudharta.ac.id

Abstract−Eye disease are visual impairments that can lead to blindness if not detected early. Fundus imaging is one of the most effective methods for identifying abnormalities in the eye. With the advancement of deep neural network technologies, particularly Convolutional Neural Network (CNN), the classification of fundus image can now be performed efficiently. LeNet is a well-known CNN architecture commonly used in image classification tasks, however it has limitation when processing images with complex visual features with high resolution, such as fundus images. This study proposes a modification to the LeNet architecture to enhance it's a ability to extract important features from images with high resolution. The modification involves adding convolutional layers and adjusting image resolution to optimize the models performance in detecting eye disease in fundus images. The dataset used consists of 4,217 fundus images, classified into four categories: normal, cataract, glaucoma, and diabetic retinopathy. Experimental result show that the original LeNet-5 achieved an accuracy 0f 76%, while the modified LeNet architecture improved the accuracy to 86%. The main contibution of this research lies in the development of a modified and lighweight LeNet architecture, which is capable of handling high-resolution fundus images while maintainig computational efficiency and producing better classification performance compared to the original LeNet.

Keywords: CNN; LeNet; Fundus Image; Classification; Retinal Pathology

1. INTRODUCTION

The eyes are one of the most vital organs in the human body. They serve as the primary sensory tool in the visual system, enabling individuals to carry out daily activities [1], [2] Eye ddiseases are disorders that affect the visual organs and can significantly impact a person's quality of life. Common types of eye diseases include cataract, glaucoma, and diabetic retinopathy[3]. Cataract occur when the eye's lens becomes cloudy, resulting in blurred or hazy vision[4], [5]. Glaucoma is a chronic eye disease caused by increased intraocular pressure which can risk the optic nerve and the lead to permanent blindness if left untreated[1], [6]. Diabetic retinopathy, on the other hand, is a effect of diabetes that make the impact to the vessels of the retina and can cause gradual vision loss[7], [8].

According to data from the World Health Organization (WHO), in a report released on world Sight day 2019, approximately 2.2 billion people worldwide suffer from vision impairment, with nearly 50% of them experiencing total blindness[9], [10]. This figure highlights that visual impairment is a serious global health issue that should not be overlooked. One of the main reasons for the hight rate of blindness is the lack or early awareness among patients regarding visual problems. As a result, treatment for eye diseases such as cataract, glaucoma, and diabetic retinopathy is often delayed[11].

Fundus images are the most commonly used type of medical images for detecting eye disorders[12], [13]. Fundus image is a visual representation of the posterior segment of the eye, captured using a specialized instrument known as a fundus camera. It reveals critical anatomical structures, including the retina, retinal blood vessels, and the macula[14]. Eye diseases such as cataract, glaucoma, and diabetic retinopathy are examples of conditions that can be identified using fundus imagery[15], [16]. However, diagnosing eye diseases due to the hight visual complexity of retinal structures and the often-similar symptoms among different types of eye conditions[17], [18]. Therefore, a system capable of classifying fundus images quickly and accurately is essential to support the early detection of eye diseases[19]. One effective approach to address this task is the application of deep learning, particularly Convolutional Neural Networks (CNN), which have proven capable of automatically recognizing complex visual patterns[20].

In addition to CNN-based approaches, conventional techniques have also been applied to fundus image classification. A study conducted by [21] proposed a machine learning-based method for retinal fundus image classification using Sobel segmentation for edge extraxtion, Hu Moments for feature representation, and a Linear Support Vector Classifier (SVC) to distinguish four classes of eye condition. The experimental results reported an accuracy of 44,34%, indicating that traditional feature extraxtion methods combined with linear classifiers still face limitations in effectively capturing the complex visual chaacteristics of fundus images. On the other hand, deep learning-based approaches for eye disease classification have been explored [20] by comparing the DenseNet and EfficientNetB3 architectures for classifying retinal fundus images into four categories. The experimental results demonstrated that efficienNetB3 achieved the highest accuracy of 95%, outperforming DenseNet. However, the architectures employed are considered complex CNN models with a large number of parameters, resulting in high computational requments and reduced efficiency when imlemented on systems with limited resources.

One of the most popular and efficient CNN architectures is LeNet, known for its simplicity and effectiveness in pattern recognition tasks[22], [23]. However, LeNet was originally designed for the MNIST dataset, which consists of low-resolution images. As a result, LeNet has limitations when processing high-resolution and complex image such as fundus images. Reducing fundus images to fit LeNet original input size can lead to the loss of important visual

BULLETIN OF COMPUTER SCIENCE RESEARCH
ISSN 2774-3659 (Media Online)
Vol 6, No 2, February 2026 | Hal 585-593
https://hostjournals.com/bulletincsr
DOI: 10.47065/bulletincsr.v6i2.796

information, including small features that are crucial for detecting eye diseases. Therefore, this study proposes a modified LeNet architecture to improve accuracy in fundus image classification.

Although prior studies[24] demonstrate that modified LeNet architectures improve medical image classification such as in breast cancer ultrasound analysis, these adaptations remain unexplored for high-resolution fundus imagery. To bridge this gap, we propose a novel LeNet-based architecture specifically engineered for retinal image classification. Therefore, this study aims to develop and evaluate a modified LeNet architecture, a lighweight and efficient CNN model designed to improve the classification performance of high-resolution retinal fundus images while maintaining low computational complexity. In addition, this study seeks to investigate the effectiviness of the proposed architecture incapturing fine-grained pathological features and to compare its performance with conventational LeNet and more complex deep learning models, thereby providing an efficient alternative for accurate eye disease classification in resource- constrained environments.Our key contributions include: 1. Structural modifications to the original LeNet framework enabling efficient processing of high-resolution fundus images without sacrificing critical features; 2. Optimization for detecting subtle pathological patterns in complex retinal structures; and 3. Enhanced accuracy in classifying cataract, glaucoma, and diabetic retinopathy. By preserving fine-grained details lost during downscaling in standard LeNet, our model offers a clinically viable tool for early diagnosis, addressing the global challenge of preventable blindness.

2. RESEARCH METHODOLOGY

This study uses a public fundus image dataset categorized into cataract, glaucoma, diabetic retinopathy, and normal classes. Images undergo preprocessing including resizing and augmentation. A modified LeNet architecture with additional convolutional layers and is implemented. The general pipeline as shown in Figure 1

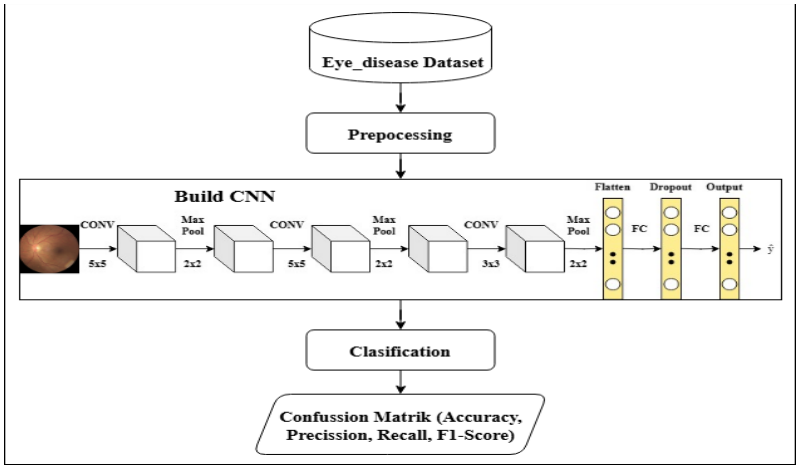

Figure 1. Research Flow

2.1 Dataset

One of the main factors contributing to vision loss is retinal disease, which can be detected through fundus imaging. Early detection of eye disease is crucial to assist doctors in making accurate and efficient diagnoses and treatment decisions. This study analyzed four eye conditions Normal, Glaucoma, Cataract, and Diabetic Retinopathy that can seriously impact vision if left untreated. Examples of eye conditions identified by fundus imaging are shown in Figure 2

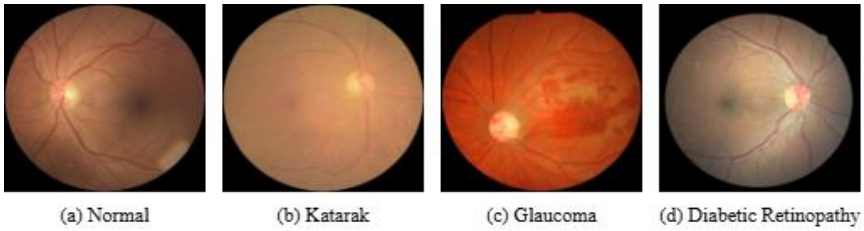

Figure 2. Example Dataset

Figure 2 presents a visual illustration of the four categories of eye conditions used as the study data, with each fundus image highlighting the characteristics of each class. In the Normal class, the image shows a retina with clearly visible blood vessel structures, a well-defined optic disc, and no abnormalities, indicating a healthy eye. In the Glaucoma class, the fundus image shows changes in the optic disc characterized by a significant increase in the cup-to-disc ratio, which is characteristic of optic nerve damage due to increased intraocular pressure. In the Cataract class, the image appears hazy or foggy with reduced contrast, making retinal structures less visible; this is due to lens opacities that block

BULLETIN OF COMPUTER SCIENCE RESEARCH
ISSN 2774-3659 (Media Online)
Vol 6, No 2, February 2026 | Hal 585-593
https://hostjournals.com/bulletincsr
DOI: 10.47065/bulletincsr.v6i2.796

light from reaching the retina. Meanwhile, in the Diabetic Retinopathy class, the image shows hemorrhagic spots, hard, yellowish-white exudates, and microaneurysms along the retinal blood vessels, which are the result of blood vessel damage.

The data used in this study were obtained from Kaggle.com[25], which consists of 4,217 fundus images categorized into four classes and used to build and learn the Modified LeNet model. The data distribution is shown in Table 1.

Table 1. Number of Dataset

Class	Amount
Normal	1074
Glaucoma	1007
Cataract	1038
Diabetic Rethinopathy	1098
Total	4217

2.2 Data Prepocessing

The preprocessing pipeline was designed to enhance model performance and robustness. First, all fundus images were resized to standardize dimensions and optimize computational efficiency. Next, pixel values were normalized to a (0,1), followed by standardization with dataset-specific mean and standard deviation values. To address data scarcity and improve generalization, augmentation techniques including random horizontal flips and color jitter (brightness/contrast variations. These steps collectively mitigate overfitting risks while ensuring invariance to rotational and illumination changes.

a. In this study, all images were resized to 256×256 pixels to ensure uniform dimensions and reduce computational complexity during the classification process.
b. The normalization process aims to standardize the data scale and accelerate the training process. In the context of fundus image classification using CNN, normalization is applied to pixel values that have been scaled to the (0,1) range using ToTensor (). After that, each pixel value is normalized to a standard distribution based on the mean and standard deviation of 1.
a. Data augmentation performed to increase the variation in the dataset by applying several transformations to the original images. This process also helps to minimize the overfitting[6], [26], and make the models generalization more better. Data augmentation used in this study include :
    1. Random Horizontal Flip, this technique randomly flips the image horizontally. It helps the model learn to recognize object regardless of their left-right orientation.
    2. Random Rotation, images are randomly rotated up to ± 180 degrees. This enhances the models robustness to rotational variance in the input images.
    3. Color Jitter, this method randomly alters the images color attributes such as brightness and contrast. It is intended to help the model recognize images under different lighting conditions.

All augmentation process were implemented using the transform function from the transform function from the Thorchvision library, which applies random transformations to images during the training phase. The example of the augmented retinal fundus images is shown in figure 2.

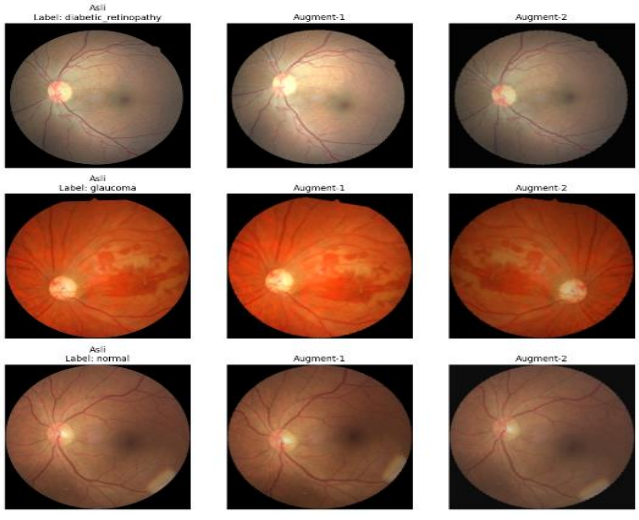

Figure 3. Augmentation Example

2.3 Modified LeNet Architecture

The layer arrangement of the modified LeNet architecture is presented in illustrated in Figure 3.

BULLETIN OF COMPUTER SCIENCE RESEARCH
ISSN 2774-3659 (Media Online)
Vol 6, No 2, February 2026 | Hal 585-593
https://hostjournals.com/bulletincsr
DOI: 10.47065/bulletincsr.v6i2.796

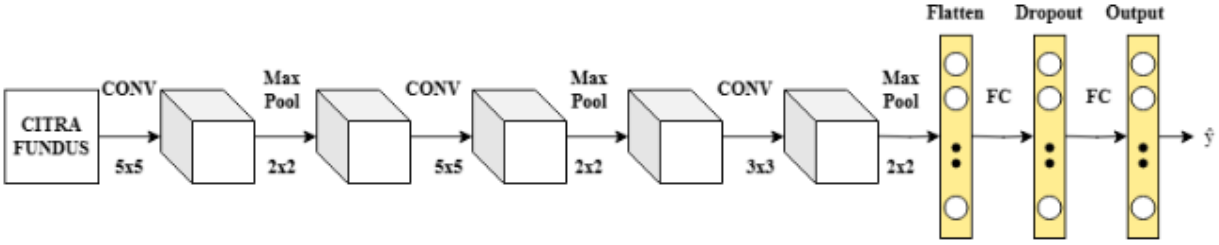

Figure 4. Architecture LeNet Modified

Based on the structure of the Convolutional Neural Network (CNN) using the modified LeNet architecture, the model consist of three convolutional layers. The first two layers use filters of size 5×5, while the third layer uses a 3×3 filter. The number of filters used in each layer is 6, 16, and 32, respectively, arranged from fewer to more filters. This incremental pattern is intended to gradually extract more complex features from the input images.

In this architecture, the stride value is not explicitly defined, so the default stride of 1 is applied, meaning the filter moves one pixel at a time during convolution. After each convolutional layer 2×2 MaxPooling operation is performed to reduce computational complexity and the risk of overfitting. Each convolutional layer is also followed by a Dropout layer with a rate of 0,25 as a regularization technique, randomly deactivating a portion of neurons during training to prevent overfitting.

After completing the three convolutional and pooling layers, the extracted features are flattened into a one-dimensional vector using a Flatten layer. The process then continues to the Fully Connected (Dense) layers, consisting of three layers with 120, 84, and 4 neurons, respectively. ReLu activation is applied to the first two Dense layers to introduce non-linearity, while the final layer outputs prediction for four classes.

The addition of convolutional layers in the modified LeNet architecture increases the model's representational capacity. The increased number of filters and layers allows the network to capture more complex features, from low-level edges to high-level retinal structures. The choice of filter sizes (5x5 and 3x3) is theoretically based on a balance between local receptive fields, which detect fine-grained vascular patterns, and broader contexts that capture pathological regions.

The use of dropout is theoretically supported as a regularization technique, which introduces stochasticity into the training process and reduces neuronal co-adaptation. This improves model generalization by minimizing overfitting; max-pooling reduces dimensionality while preserving dominant features, which is mathematically analogous to a local nonlinear downsampling operator. Together, these modifications theoretically explain why the proposed model can handle the high-resolution nature of fundus images more effectively than the original LeNet.

One of the approach used in this study is the Cross Entropy Loss function, which is employed to measure the difference between the true labels and the models predicted outputs. Cross Entropy Loss is particularly well-suited for classification classes.

This loss function work by comparing the predicted probability distribution (p) with the true labels (y), and calculating the loss when the models prediction deviate from the correct labels. The closer the prediction are to the true labels, the smaller the resulting loss value. The formula for Cross Entropy Loss is as Eq1.

$$-N1\Sigma i = 1N\Sigma j = 1C(yi, j.log(pi, j)) \quad (1)$$

2.4 Training and Testing

The classification process was carried out using a Convolutional Neural Network (CNN) model designed base on the modified LeNet architecture. The model was optimized using the Adam optimization of algorithm, which make the better efficiency and more effective of the training process.

The dataset is split into training and testing sets using a random split of 80:20. The 80% training data is used to train the model to recognize image patterns, while the remaining 20% is used to evaluate the model performance.

Experiments were conducted in stages by applying variations to parameters such as image size, learning rate, and number of epochs. The purpose of these variations to parameter on the model performance and to identify the best configuration that yields optimal classification results.

2.4 Evaluation

The confusion matrix evaluates the best model performance in classifying fundus images by quantifying correct/incorrect predictions, with the following performance metrics calculated: precision (Equation 2), accuracy (Equation 3), recall (Equation 4), and F1 score (Equation 5). This matrix is also used to evaluate the relationship between positive and negative classes. Table 3 presents the evaluation matrix.

$$Accuracy = \frac{TP+TN}{TP+TN+FP+FN} \quad (2)$$

$$Precision = \frac{TP}{TP+FP} \quad (3)$$

$$Recall = \frac{TP}{TP+FN} \quad (4)$$

BULLETIN OF COMPUTER SCIENCE RESEARCH
ISSN 2774-3659 (Media Online)
Vol 6, No 2, February 2026 | Hal 585-593
https://hostjournals.com/bulletincsr
DOI: 10.47065/bulletincsr.v6i2.796

$$F1 - Score = 2 \times \frac{Precision \times Recall}{Precision + Recall} \quad (5)$$

Table 2. Confussion Matrix

		Actual value	
		Positif	negatif
Prediction value	Positif	True positif	False positif
	Negatif	False negatif	True negatif

Table 2 presents the classification results based on four terms: True Positive (TP) refer to positive instances that were correctly predicted. False Positive (FP) refer to negative instances that were incorrectly classified as positive. True Negative (TN) refer to negative instances that were correctly predicted. False Negative (FN) refer to positive instances that were incorrectly classified as negative.

3. RESULT AND DISCUSSION

This study successfully developed a fundus image-based eye disease classification model using a modified LeNet architecture. The model was designed to identify four categories of eye conditions from digital fundus images. After undergoing training and evaluation, the modified model demonstrated strong performance in distinguishing healthy eyes from those with disease indications. The results are visualized through accuracy and loss curves during training, a confusion matrix, and evaluation metrics such as precision, recall, and F1-score.

The evaluation outcomes indicate that the modified LeNet architecture outperforms the original LeNet, both in terms of accuracy and robustness against variations in fundus images. This finding highlights that adjustments to the LeNet architecture can significantly enhance the model's ability to detect eye diseases in fundus images. Moreover, the study provides a reliable solution to support faster, more accurate, and efficient eye disease screening, thereby contributing to early detection in the field of ophthalmology.

The fundus image dataset was divided into two main subsets: training and testing, with an 80:20 ratio. Specifically, 80 percent of the data was used to train the model to learn the visual patterns of each disease class, while the remaining 20 percent was used to test the model's ability to generalize to unseen data. This partitioning strategy was employed to prevent overfitting while maintaining a balance between learning and evaluation.

3.1 Evaluation

This study involved several stages of model evaluation using a Convolutional Neural Network (CNN) with the LeNet architecture. The experiments were conducted using different variation, including the original LeNet and a Modified version. Additional test were performed by varying image sizes, learning rate, number of epochs, and optimizer. All experiment were carried out using the pre-processed fundus image dataset, aiming to evaluate the impact of each parameter on the models performance in classifying eye diseases.

Table 3. Performance Comparison Between Standard LeNet-5 and Modified LeNet Architectures

	LeNet 5 (Original)	LeNet Modifikasi
Accuracy	76	83
Precission	76	83
Recall	76	83
F1-Score	76	83
Loss	59	62

Based on Table 3, experiments were conducted using the Lenet Original LeNet-5 architecture and the modified LeNet. The original LeNet-% achieved an accuracy, precision, recall, and F1-Score of 76%. These results showing that the model performs reasonably well, although there is still room for improvement, particularly in its ability to recognize patterns in fundus images.

The testing results of the modified LeNet showed an improvement in model performance, with accuracy, precision, recall, F1-Score increasing to 83%. This enhancement in evaluation metrics demonstrates that the modified architecture provides better feature representation and improved stability in classifying fundus image.

According to statistical learning theory, a deeper architecture increases the model's hypothesis space, allowing it to approximate more complex functions. In this case, the original LeNet with two convolutional layers had limited capacity to extract discriminative retinal patterns. By adding additional convolutional layers and optimizing the kernel size, the model effectively reduced bias and improved feature representation, explaining the accuracy increase from 76% to 83%.

The next experiment was conducted to evaluated the impact of image size on model performance. Image size is an important factor in training a CNN model, as it affects the amount of information the model receives. In this test, four different image sizes were used : 64×64, 128×128, 224×224, and 256×256 pixels. All training process used the Adam optimizer, a learning rate of 0.001, and 50 epochs. Table 4 presents the evaluation result for each image size.

BULLETIN OF COMPUTER SCIENCE RESEARCH
ISSN 2774-3659 (Media Online)
Vol 6, No 2, February 2026 | Hal 585-593
https://hostjournals.com/bulletincsr
DOI: 10.47065/bulletincsr.v6i2.796

Table 4. Model Performance Across Different Input Image Resolutions

Size Image	64×64	128×128	224×224 px	256×256 px
Accuracy	83	84	84	86
Precission	83	83	83	85
Recall	83	83	83	85
F1-Score	83	83	83	85
Loss	42	45	49	42

Based on the results in Table 4, large image sizes yielded better model performance. The 256×256 pixel size produced the highest results, with an accuracy, of 86% and precision, recall, and F1-Score all reaching 85%. This indicates that larger image size allow the model to capture more detailed feature information, which enhances classification capability. However, increasing image size should be balanced with available computational resources, as larger inputs require more processing power.

In addition, testing was conducted to evaluate the impact of varying learning rates on model performance. In this experiment, the model trained using the Adam optimizer, with an image size of 256×256 pixels and 50 epoch. Table 5 presents the results of the models performance across four different learning rate values:

Table 5. Model Performance Across Different Learning Rate

Learning Rate	0,01	0,001	0,0001	0,00001
Accuracy	24	86	81	67
Precission	19	85	81	68
Recall	25	85	81	67
F1-Score	12	85	81	67
Loss	1.39	42	45	76

Based on the results in table 5, the learning rate of 0.001 provided the best performance, whit an accuracy of 86%, precision, recall, and F1-Score each at 85%, and loss value of 42%. A learning rate that is to high, such as 0.01, resulted in very poor performance and a high loss value of 1.39, indicating that the model struggled to learn effectively. On the other hand a learning rate that is too low, such as 0.00001, also led to suboptimal performance due to an excessively slow training process, as indicated by an accuracy and F1-Score of only 67%. Therefore, selecting an appropriate learning rate is crucial for the achieving optimal model performance. In this case, a learning rate of 0.001 was the most effective configuration for the given architecture and dataset.

This experiment was conducted to evaluate the impact of the number of epochs on model performance in fundus image classification. An epoch refers to one complete iteration over the entire training dataset during the model training process. In this test, the model was trained using image size of 256×256 pixels. The model was evaluated using three different epoch setting 30, 50, 70 epochs. The result are presented in table 6.

Table 6. Model Performance Across Different Epoch

Epoch	30	50	70
Accuracy	83	86	85
Precission	82	85	85
Recall	82	85	85
F1-Score	82	85	85
Loss	41	42	63

Based on Table 6, the model achieved its best performance at epoch, with an accuracy of 86% and precision recall, and F1-Score all at 85%. Although the main metrics remained high and stable at 70 epoch, the loss value increased to 63%. Which may indicate the onset overfitting. At 30 epoch, the metrics were already reasonably good (around 82-83%), but slightly lower compared to the performance at 50 epoch. Generally, increasing the number of overfitting if no significant improvement is achieved after a certain point.

This experiment aimed to evaluate the impact of different optimizer on model performance. Optimizer play a crucial role in updating model weights during training and influence both the convergence speed and the final model quality. In this experiment, four optimizers were compared : SGD, Adagrad, Adam, and RMSprop. All tests were conducted using the same parameters : image size of 256×256 pixels, learning rate of 0.001, and 50 epochs. Table 7 presents the performance evaluation results for each optimizer.

Table 7. Model Performance Across Different Optimizer

Optimizer	SGD	Adagrad	Adam	RMSprop
Accuracy	64	77	86	86
Precission	63	77	85	87
Recall	63	75	85	86
F1-Score	59	75	85	86

BULLETIN OF COMPUTER SCIENCE RESEARCH
ISSN 2774-3659 (Media Online)
Vol 6, No 2, February 2026 | Hal 585-593
https://hostjournals.com/bulletincsr
DOI: 10.47065/bulletincsr.v6i2.796

Optimizer	SGD	Adagrad	Adam	RMSprop
Loss	83	55	42	51

Based on Table 7, the Adam and RMSprop optimizers achieved the highest accuracy at 86%. However, Adam yielded the lowest loss value at 42, indicating better training stability. Adagrad showed decent performance with an accuracy of 77%, but still feel short compared to Adam and RMSprop. SGD produced the lowest overall performance in term of accuracy, F1-Score , and had the highest loss value at 83. Adam outperformed other optimizer techniques, enabling a more stable and efficient training process.

From the entire series of experiments conducted, it can be concluded that the best performance was achieved by using a CNN model with a modified LeNet architecture, an image size of 256×256 pixels. This configuration resulted in the highest performance, with accuracy of 86%, precision of 85%, recall of 85%, and an F1-Score of 85%.

These results demonstrate that the modified LeNet architecture is more effective than the original version in capturing important features from high-resolution fundus images. Moreover, using the right parameter configuration plays a significant role in improving the model accuracy and training stability.

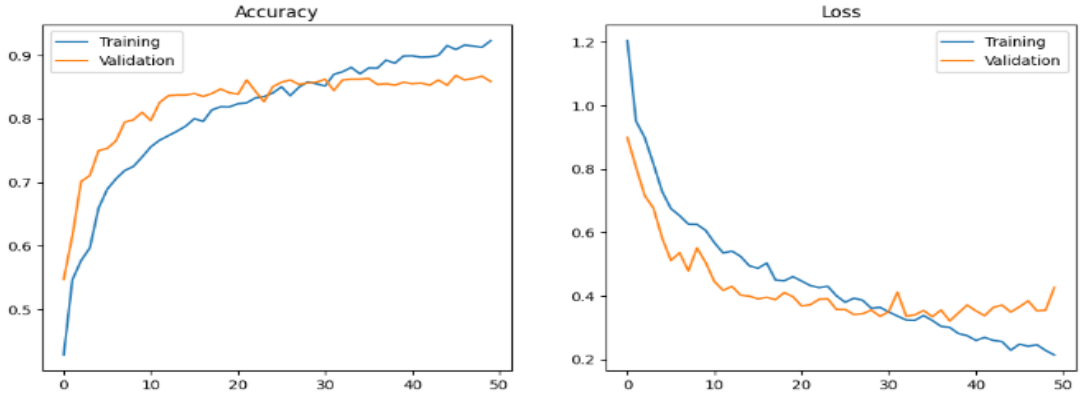

Figure 5. Line Plot Accuracy and Loss

Figures 5 illustrate the accuracy and loss graphs throughout the model training process for retinal pathology classification in fundus images.

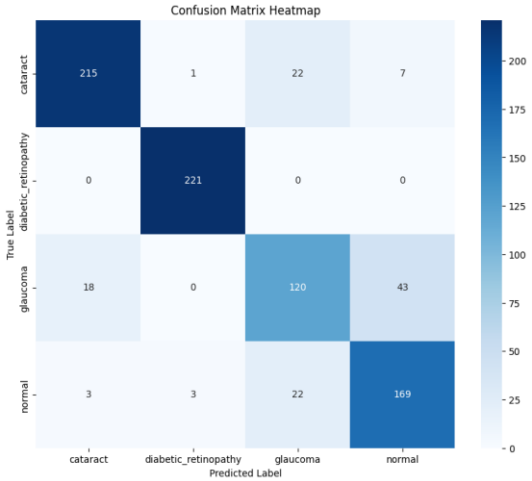

Figure 6. Confussion Matrix Result

Classification Report

	precision	recall	f1-score	support
cataract	0.91	0.88	0.89	245
diabetic_retinopathy	0.98	1.00	0.99	221
glaucoma	0.73	0.66	0.70	181
normal	0.77	0.86	0.81	197
accuracy			0.86	844
macro avg	0.85	0.85	0.85	844
weighted avg	0.86	0.86	0.86	844

Figure 7. Classification Report

BULLETIN OF COMPUTER SCIENCE RESEARCH
ISSN 2774-3659 (Media Online)
Vol 6, No 2, February 2026 | Hal 585-593
https://hostjournals.com/bulletincsr
DOI: 10.47065/bulletincsr.v6i2.796

Figure 6 and 7 presents the evaluation of the eye disease classification model based on fundus images using the confussion matrix and classification report. The confussion matrix ilustrates the distribution model of the models prediction occross four class. From the heatmap visualization, it can be observed that most prediction lie along the main diagonal, indicating strong alignment between the actual and predicted labels. Out of a total of 844 images used for testing, 725 image were correctly classified, while 119 images were misclassified.

The classification report provides evaluation metrics in terms of precission, recall, and F1-score for each class. The best performance was achieved in the Diabetic Retinopathy class, with a recall of 100% and an F1-score of 0,99, highlighting the models excellent ability recognize this condition. In contrast, the lowest performance was observed in the Glaicoma class, with a precission of 0.73 and recall off 0.66, indicating several missclassification.

3.2 Classification Result

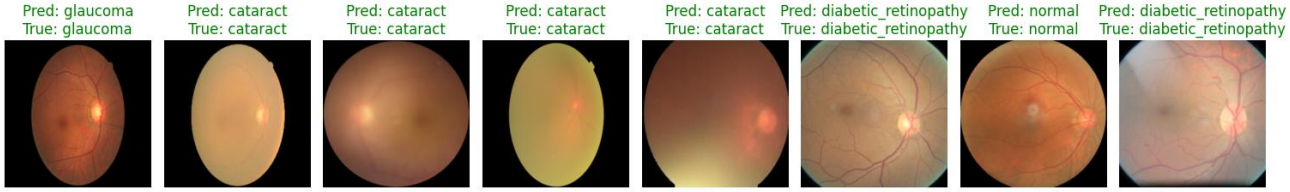

Figure 8. Correctly Classified Images

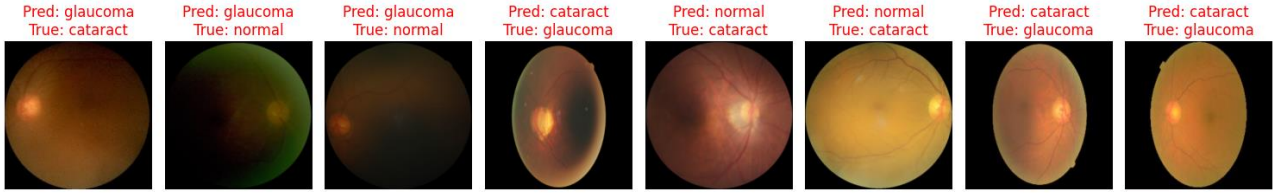

Figure 9. Incorrectly Classified Images

Figure 8 and 9 ilustrates the evaluation results the eye disease classification model based on fundus images using the modified LeNet architecture. Overall, the predictions show consistency between the actual and predicted labels, with a relatively high level of confidence. The proposed model achieved good performance, particulary in the diabetic retinopathy class, which was predicted with a recall of 100% and F1-score 0f 0,99.

However, some misclassifications were still observed. For instance, in the normal class, the model occasionally misclassified images as Glaucoma with a lower probability, as shown in the confussion matrix. A similar case occurred in the Cataract class, wich was sometimes predicted as another class. Nevertheless, the model maintained a strong overall performance acjieving am average accuracy of 86%.

These missclassifications indicate that certain eye conditions, such as Normal and laucoma, share similar visual characteristics in fundus images, which can cause confussion for the model.overall, the prediction results confirm that the modified LeNet achitecture delivers strong performance, though there remains room for improvement, particularly in distinguishing between classes with similar features.

4. CONCLUSION

The challenge of classifying fundus images, particularly in distinguishing between eye diseases such as cataract, glaucoma, diabetic retinopathy, and normal conditions, was successfully addressed by applying a modified CNN LeNet architecture. The experiments were conducted using a public fundus image dataset under various model configurations, including image size variations, number of epoch, optimizer type, learning rate, and the application of augmentation. The best performance was achieved with the combination of 256×256 image size, Adam optimizer, LR 0.001, and training epoch 50, yielding an accuracy of 86%, precision of 85%, recall of 85%, and F1-Score 85%. The confusion matrix revealed that the majority of images were correctly classified, particularly in the diabetic retinopathy and cataract classes. This performance improvement is crucial in supporting early detection of eye diseases, which plays a vital role in preventing blindness and enhancing patients quality of life. Moreover, the automated classification system can serve as an effective decision-support tool for medical professionals in diagnosing eye condition. Hese improvements are consistent with the theoretical foundations of CNNs, where deeper convolutional layers enhance the hierarchical extraction of visual patterns, and larger input resolutions preserve fine-grained retinal features essential for pathology detection. the inclusion of dropout regularization theoretically reduces overfitting, leading to improved generalization on unseen data. Thus, the proposed modification of LeNet is not only empirically effective but also theoretically justified as a lightweight yet capable architecture for fundus image classification. These efforts are expected to lead to the development of a more accurate and reliable eye disease classification system. Although the modified LeNet model demonstrated strong performance, further improvements are still necessary. Some classes, such as glaucoma, continue to

show relatively high misclassification rates. Future research is recommended to explore additional regularization techniques (such early stopping or deeper dropout), automated hyperparameter optimization, and more diverse augmentation strategies. Furthermore, employing more advanced CNN architectures and evaluating the model on larger and more diverse fundus image dataset could significantly enhance model generalization.

REFERENCES

[1] A. Tashkandi, "Eye Care: Predicting Eye Diseases Using Deep Learning Based on Retinal Images," *Computation*, vol. 13, no. 4, p. 91, Apr. 2025, doi: 10.3390/computation13040091.
[2] O. Bernabe, E. Acevedo, A. Acevedo, R. Carreno, and S. Gomez, "Classification of Eye Diseases in Fundus Images," *IEEE Access*, vol. 9, pp. 101267–101276, 2021, doi: 10.1109/ACCESS.2021.3094649.
[3] E. H. Rachmawanto *et al.*, "Eye disease classification using deep learning convolutional neural networks," *J. Soft Comput. Explor.*, vol. 5, no. 4, pp. 332–341, Dec. 2024, doi: 10.52465/joscex.v5i4.493.
[4] R. Amin, A. Ahmed, S. Shabih Ul Hasan, and H. Akbar, "Multiple Eye Disease Detection Using Deep Learning," *Found. Univ. J. Eng. Appl. Sci. Bri StylecolorblackHEC Recognized Categ. ISSN 2706-7351i*, vol. 3, no. 2, pp. 14–26, Jan. 2023, doi: 10.33897/fujeas.v3i2.689.
[5] G. Sharma, V. Anand, and S. Gupta, "Cracking Light on Cataract Detection by Implementing VGG16 Transfer Learning-Based Model on Fundus Images," in *2023 International Conference on Research Methodologies in Knowledge Management, Artificial Intelligence and Telecommunication Engineering (RMKMATE)*, Chennai, India: IEEE, Nov. 2023, pp. 1–6. doi: 10.1109/rmkmate59243.2023.10368860.
[6] A. Shoukat, S. Akbar, S. A. Hassan, S. Iqbal, A. Mehmood, and Q. M. Ilyas, "Automatic Diagnosis of Glaucoma from Retinal Images Using Deep Learning Approach," *Diagnostics*, vol. 13, no. 10, p. 1738, May 2023, doi: 10.3390/diagnostics13101738.
[7] B. Menaouer, Z. Dermane, N. El Houda Kebir, and N. Matta, "Diabetic Retinopathy Classification Using Hybrid Deep Learning Approach," *SN Comput. Sci.*, vol. 3, no. 5, p. 357, Jul. 2022, doi: 10.1007/s42979-022-01240-8.
[8] K. V. Naveen, B. N. Anoop, K. S. Siju, M. K. Kar, and V. Venugopal, "EffNet-SVM: A Hybrid Model for Diabetic Retinopathy Classification Using Retinal Fundus Images," *IEEE Access*, pp. 1–1, 2025, doi: 10.1109/ACCESS.2025.3566073.
[9] "Vision impairment and blindness." Accessed: Jul. 24, 2025. [Online]. Available: https://www.who.int/news-room/fact-sheets/detail/blindness-and-visual-impairment
[10] S. Benbakreti, S. Benbakreti, and U. Ozkaya, "The classification of eye diseases from fundus images based on CNN and pretrained models," *Acta Polytech.*, vol. 64, no. 1, pp. 1–11, Mar. 2024, doi: 10.14311/AP.2024.64.0001.
[11] R. Sarki, K. Ahmed, H. Wang, Y. Zhang, and K. Wang, "Convolutional Neural Network for Multi-class Classification of Diabetic Eye Disease," *ICST Trans. Scalable Inf. Syst.*, p. 172436, 2021, doi: 10.4108/eai.16-12-2021.172436.
[12] O. Ouda, E. AbdelMaksoud, A. A. Abd El-Aziz, and M. Elmogy, "Multiple Ocular Disease Diagnosis Using Fundus Images Based on Multi-Label Deep Learning Classification," *Electronics*, vol. 11, no. 13, p. 1966, Jun. 2022, doi: 10.3390/electronics11131966.
[13] R. Mohan, S. Kadry, S. Yassine, and V. Rajinikanth, "Healthy/Glaucoma Fundus Retinal Image Classification using Butterfly Algorithm Optimized ResNet-Features," *Procedia Comput. Sci.*, vol. 258, pp. 1804–1812, 2025, doi: 10.1016/j.procs.2025.04.432.
[14] T. Hu, B. Yang, W. Zhang, Y. Zhang, and H. Li, "A degradation-aware enhancement network with fused features for fundus images," *Expert Syst. Appl.*, vol. 266, p. 125954, Mar. 2025, doi: 10.1016/j.eswa.2024.125954.
[15] C. Guo, M. Yu, and J. Li, "Prediction of Different Eye Diseases Based on Fundus Photography via Deep Transfer Learning," *J. Clin. Med.*, vol. 10, no. 23, p. 5481, Nov. 2021, doi: 10.3390/jcm10235481.
[16] J. Wang, L. Yang, Z. Huo, W. He, and J. Luo, "Multi-Label Classification of Fundus Images With EfficientNet," *IEEE Access*, vol. 8, pp. 212499–212508, 2020, doi: 10.1109/access.2020.3040275.
[17] A. Shamsan, E. M. Senan, and H. S. A. Shatnawi, "Automatic Classification of Colour Fundus Images for Prediction Eye Disease Types Based on Hybrid Features," *Diagnostics*, vol. 13, no. 10, p. 1706, May 2023, doi: 10.3390/diagnostics13101706.
[18] L. Hakim, "Regularizer based on Euler characteristic for retinal blood vessel segmentation," *Pattern Recognit. Lett.*, vol. 149, 2021, doi: doi:10.1016/j.patrec.2021.05.023.
[19] N. Al-Kahtani, J. Varela-Aldás, A. Aljarbouh, M. K. Ishak, and S. M. Mostafa, "Discrete migratory bird optimizer with deep transfer learning aided multi-retinal disease detection on fundus imaging," *Results Eng.*, vol. 26, p. 104574, Jun. 2025, doi: 10.1016/j.rineng.2025.104574.
[20] C. Jatmoko, H. Lestiawan, F. Agustina, and L. Erawan, "Comparative Study of Classification of Eye Disease Types Using DenseNet and EfficientNetB3," *Kinet. Game Technol. Inf. Syst. Comput. Netw. Comput. Electron. Control*, Jul. 2024, doi: 10.22219/kinetik.v9i3.1931.
[21] F. T. A. Sayyidul Laily, "Feature Extraction and Classification of Retinal Images Using Sobel Segmentation and Linear SVC," *Int. J. Artif. Intell. Med. Issues*, vol. 2, no. 2, pp. 136–149, Nov. 2024, doi: 10.56705/ijaimi.v2i2.153.
[22] Md. R. Islam and A. Matin, "Detection of COVID 19 from CT Image by The Novel LeNet-5 CNN Architecture," in *2020 23rd International Conference on Computer and Information Technology (ICCIT)*, DHAKA, Bangladesh: IEEE, Dec. 2020, pp. 1–5. doi: 10.1109/ICCIT51783.2020.9392723.
[23] X. Chen and R. Hu, "Intelligent English multiple-choice question scoring method based on LeNet-5 and strengthened convolutional module," *Syst. Soft Comput.*, vol. 7, p. 200314, Dec. 2025, doi: 10.1016/j.sasc.2025.200314.
[24] S. Balasubramaniam, Y. Velmurugan, D. Jaganathan, and S. Dhanasekaran, "A Modified LeNet CNN for Breast Cancer Diagnosis in Ultrasound Images," *Diagnostics*, vol. 13, no. 17, p. 2746, Aug. 2023, doi: 10.3390/diagnostics13172746.
[25] "penyakit_mata." Accessed: Jul. 25, 2025. [Online]. Available: https://www.kaggle.com/datasets/annisawlya/penyakit-mata
[26] A. Nawaz, T. Ali, G. Mustafa, M. Babar, and B. Qureshi, "Multi-Class Retinal Diseases Detection Using Deep CNN With Minimal Memory Consumption," *IEEE Access*, vol. 11, pp. 56170–56180, 2023, doi: 10.1109/ACCESS.2023.3281859.